Hindawi
Shock and Vibration
Volume 2022, Article ID 2539870, 11 pages
https://doi.org/10.1155/2022/2539870

Research Article

Modal Investigation on a Large-Scale Containership Model for Hydroelastic Analysis

Ye Lu,[1] **Juan Liu**,[2] **Bei Teng**,[3] **Chao Tian**,[1] **Hailong Si**,[1] **Qingyun Zhou**,[1] **and Xinyun Ni**[1]

[1]*China Ship Scientific Research Center, Wuxi 214082, China*
[2]*Jiangsu University of Science and Technology, Zhenjiang 212003, China*
[3]*Wuxi Institute of Communications Technology, Wuxi 214151, China*

Correspondence should be addressed to Ye Lu; luye@cssrc.com.cn

Received 4 January 2022; Revised 3 February 2022; Accepted 29 March 2022; Published 30 April 2022

Academic Editor: Jialong Jiao

A 20,000 TEU containership with an overall length of about 400 m is designed as a target ship to investigate ship hydroelastic characteristics in the joint industry project (JIP) of CSSRC-20,000 TEU. A set of systematic model tests are carried out in the seakeeping wave basin of CSSRC. The large-scale ship model data for hydroelastic experiments are presented with the determination of modal features. The modal test of the containership model is the premise of the hydroelastic analysis. The test of the natural frequency and modal shape of the ship model can be used to corroborate the accuracy of the finite element modelling. A three-dimensional finite element model (FEM) of the ship is employed to carry out modal analysis in a vacuum and provide modal parameters to decide the large-scale ship model data for hydroelastic experiments. Through the analysis of hydroelasticity, the wet frequency corresponding to the motion of each elastic mode is obtained. Good agreement is achieved between the numerical results and the measurement data, particularly for the lower-order modes. Only when the numerical calculations of the dry and wet modes are consistent with the experimental results, the containership model's calculated motion responses and structural loads are comparable to the experimental results. Therefore, examining the modal tests is extremely important for hydroelastic analysis. As the input data, the FEM will be shared with JIP members for further comparative studies of linear and nonlinear hydroelastic analyses. The experiments help provide reliable and accurate benchmark model test data for comparative studies using numerical software and methods.

1. Introduction

With the development of the social economy and transportation demand, containerships have gradually grown larger and faster, and some superstandard ships have increasingly been designed and built. The total length of a containership of 20,000 TEU has reached 400 meters. The bow of the containership is relatively noticeable, and the speed is generally high. The slamming phenomenon of the ship is very obvious when sailing in the waves. The longitudinal strength of the containership hull is vital. As the size of the ship increases, the vertical rigidity and torsional rigidity of the containership hull are significantly reduced. At the same time, wave-induced vibration may occur in lower sea conditions, resulting in serious hull structural fatigue problems. Strong nonlinear characteristics are often observed in the ship wave load. Determining the nonlinear wave load of containerships is of great significance to the ship's safety and structural design.

The most famous containership S175 is the first containership standard model (1978) and is still the sole standard model used for teaching and research both at home and abroad, making it the most cited model [1–4]. Kim and Kim [5] calculated the elastic vibration and whipping of a 6,500 TEU containership and a fictitious 10,000 TEU containership based on the combination of a three-dimensional (3D) Rankine source and a 3D structural model. A combination of beam elements is used to consider the slamming of the two-dimensional (2D) generalised Wagner model Load. Senjanović et al. [6] proposed that hydroelastic analysis is the most suitable method for the rational design of containerships, and free vibration analysis is one of the most important

steps. It can be done using a one-dimensional (1D) or 3D finite element model (FEM) of ship structures. The beam model is usually used in the preliminary design stage, and the completed 3D FEM is more suitable for the final strength examination. Malenica and Derbanne [7] claimed that as the length of the ship increases, the hydroelastic structure response of ultralarge containerships is more important. The large size, nearly 400 meters between the vertical lines, results in a lower natural frequency of the structure. They also claimed that the correct modelling of the hydroelastic ship structure response and its inclusion in the overall design program is much more complicated than the assessment of the static structure response. Hirdaris et al. [8] reviewed several different fluid-structure coupling methods for the ship motions and loads. The weak nonlinear wave load is applied to the 10,000 TEU containership. The load is not only reasonable for at amidships, but also applicable at fore and aft. The prediction of wave excitation force of radiation potential and diffraction potential is more accurate when the instantaneous wet surface is considered. Ye et al. [9] used the 3D potential flow theory and the thin-walled beam theory to calculate the hydroelasticity problem of a large opening containership. The high-order isoparametric boundary element method is adopted to solve the boundary integral equation of the hydrodynamic boundary value problem, and the structure is simplified to consider the warpage. The FEM of thin-walled beams is investigated with the effects of shear and section rotation, as well as the large opening of the cargo hold and the torsion box. The numerical results are compared with the test data and both good calculation accuracy and calculation efficiency are obtained. Based on the ABS classification society regulations of the whipping and wave-induced vibration response, Lin et al. [10] took a 16,000 TEU ultra-large containership as an example and interpreted the specifications of various classification societies regarding the hydroelastic effect. The research found that the hydroelastic effect of ultralarge containerships cannot be ignored, and it has different effects on the longitudinal bending and fatigue damage of the ship. The whipping has increased the amidships' bending moment and shear force by 20%~25%. Wave-induced vibration also affects the ship. The cumulative fatigue damage increases by nearly 20%. Chen [11] studied the two effects of the insurmountable wave-induced vibration and whipping phenomenon on the hull strength caused by the longitudinal strength and fatigue strength in the design of superlarge ships. He tried to propose a method for the previously mentioned two kinds of ship mechanics in the initial stage of ship design. Regarding the method of forecasting frontier problems to solve the designer's difficulties, he pointed out the influence of various uncertain factors on the calculation. He pointed out that in the design of modern ultralarge civil ships, it is extremely important to strengthen model tests and full-scale ship experiments when the current theory cannot fully explain the coupling of wave-induced vibration and whipping and accurately separate their respective effects. It is the only way to ensure the safety of ships. Han et al. [12] introduced that the 18,000 TEU ultralarge containership has a high speed and significant bow, and the first-order natural frequency is lower than conventional ship types, which is likely to cause springing and whipping. The hydroelastic analysis is applied to discuss the impact of whipping and springing on the ultimate strength and fatigue strength of the ultralarge containership structure. Taking the 18,000 TEU ultralarge containership as the research object, Zhang et al. [13] considered the effects of symmetric and antisymmetric modes and used the FE method for dry modal analysis. Based on the 3D linear hydroelasticity theory in the frequency domain and spectral analysis method, the hot spot stress responses are solved. Combined with the linear cumulative damage method, the fatigue life and the influence of wave-induced vibration on the fatigue of hatch corners are obtained. It is found that wave-induced vibration will cause a high-frequency response of loads and stresses. The fatigue cumulative damage of the hatch corners has increased significantly, and the fatigue life has been reduced by up to 50%.

In addition to the previously mentioned scholars' detailed analysis and research on the hydroelasticity of containerships, many authors reviewed the research in recent years [14–16]. They carried out a detailed analysis of the external loads such as wave-induced springing on the hydroelasticity of the ship, especially the containership, and also gave the motion response and structural load evaluation caused by slamming.

From 2005 to 2009, the KCS initiated by MOERI (Maritime & Ocean Research Institute) compared the test results of tankers, containerships, and surface ships to standardize the capabilities of different ship manipulation simulation methods (based on CFD methods) test.

The international joint industrial project WILS (Wave Induced Loads on Ships) I (2006~2008), II (2008~2011), and III (2012~2014) were initiated and led by MOERI. Taking 6750 TEU and 10,000 TEU containerships, a series of studies were performed, including wave loads, modal tests, hydroelastic response, linearity and nonlinearity, full-scale ship tests, and so on.

From 2009 to 2012, Bureau Veritas (BV) initiated the TULCS (Tools for Ultra Larger Container Ship) international joint industrial project to conduct numerical calculations and experimental comparative studies on wave-induced vibration and slamming-induced whipping for 14,000 TEU containerships.

To investigate the influence of springing and whipping on the bending and torsion moments of the ship structures, a Joint Industry Project (JIP) named Comparative Study on Springing Responses of Containership 20,000 TEU (CSSRC-20,000 TEU) was initiated by Prof. Yousheng Wu from China Ship Scientific Research Center (CSSRC), which will last for about four years from 2018 to 2022. Other initiators or members of this JIP include China Classification Society (CCS), Lloyd's Register of Shipping (LR), Bureau Veritas (BV), American Bureau of Shipping (ABS), Class NK (NK), Korean Register of Shipping (KR), Indian Register of Shipping (IRS), Shanghai Waigaoqiao Shipbuilding Co. Ltd (SWS), Shanghai Merchant Ship Design & Research Institute (SDARI), University of Southampton (UoS), Chalmers University of Technology (CUT), Shanghai Jiaotong University (SJTU), Harbin Engineering University (HEU), Dalian University of Technology (DUT), Huazhong

University of Science and Technology (HUST), Wuhan University of Technology (WUT), and Jiangsu University of Technology (JUST). The initiators and members of CSSRC-20,000 TEU JIP are shown in Figure 1. The introduction to this JIP can be found on the website: jip.cssrc.com.

The objectives of this JIP contain four aspects are shown as follows:

(1) to make a global review by synthetic analysis of existing methods/software for hydroelastic analysis,

(2) to provide reliable and accurate benchmark model tests data, which can be considered as a standard database for verification and validation,

(3) to perform a comparative study of the most recent numerical methods/software by comparing with measurements of large-scaled hydroelastic model tests,

(4) to provide critical information for establishing standard procedures/guidelines for the numerical prediction of the hydroelastic response including springing and whipping.

Aiming at the main objectives of this JIP, reliable and accurate large-scale benchmark model test data [17] for comparative studies using the most recent numerical methods and software will be provided. A 20,000 TEU containership with an overall length of about 400 m has been designed as the target ship for the JIP studies, and systematic model tests have been carried out in the seakeeping wave basin of CSSRC.

In this JIP, the 3D hydroelastic method will be applied in ultralarge containerships, including linear and nonlinear methods. Based on the results of the benchmark of model test and numerical comparison, the methods adopted by the participants of this JIP will be analysed in detail. Then, the proper methods and the criterion will be advised to obtain more reasonable and accurate results.

In this paper, the modal characteristic of containership is investigated for hydroelastic analysis. As well known, based on the modal superposition, the hydroelasticity could solve the fluid-structure interaction problem easily. So, the ship modal information is demonstrated in detail including construction and the modal test. The mass distribution and stiffness distribution of the containership model settle the natural frequency of vibration in a vacuum. The manufacturing accuracy and installation method of the model can affect the frequency. During modal testing, the location of the hoisting rope and lifting point is critical, which can change the natural frequencies and modal shapes. 3D finite element numerical modelling is also very important in the connection of the ship model. A slight change in mechanical parameters such as material and elastic modulus will greatly change the natural frequency.

2. 3D Hydroelastic Method

In 1984, Yousheng Wu pioneered combining the 3D potential flow theory with the 3D structural dynamics theory to establish the 3D hydroelasticity theory. Assuming that the ship moves and deforms slightly in waves, according to the principle of modal superposition, the motion and deformation of the hull structure relative to its equilibrium position can be expressed as

Figure 1: Initiators and members of CSSRC-20,000 TEU JIP.

$$\vec{u} = \sum_{r=1}^{m} \vec{u}_r p_r = \sum_{r=1}^{m} (u_r, v_r, w_r) p_r, \quad (1)$$

where $p_r\,(r = 1, 2, \ldots, m)$ represents the r th principal coordinate component of the displacement $\vec{u}_r$ relative to the dry hull mode.

We assumed that the fluid around the floating body is an ideal fluid that is uniform and incompressible and nonviscous, the flow field had no rotation, and the free surface wave is a small amplitude wave. Combining structural dynamics, a generalised 3D linear frequency domain hydroelastic equation of motion for a floating body (1) could be obtained as follows:

$$[a + A]\{\ddot{p}\} + [b + B]\{\dot{p}\} + [c + C]\{p\} = \{Z\} + \{\Delta\} + \{Q\}. \quad (2)$$

In the formula, $[a]$, $[b]$, and $[c]$ are the generalised mass matrix, the generalised damping matrix, and the generalised stiffness matrix of the structure, respectively. Corresponding to the previously mentioned matrix, generalised fluid additional mass matrix, generalised fluid additional damping matrix, and generalised fluid restoring force matrix are $[A]$, $[B]$, and $[C]$. Moreover, $\{Z\}$, $\{\Delta\}$, and$\{Q\}$ are generalised surface force, generalised concentrated force, and generalised volume force arrays, respectively; $\{p\}$ is generalised principal coordinate arrays.

3. Ship Model

3.1. Scale and Main Particulars. The experimental model of the containership is made of steel with a two-cylinder backbone. It is divided into 14 segments connected by the flexible backbone (Figure 2). The ship model is segmented at St 2, St 4, St 5 + 50 mm, St 6, St 7, St 8.5, St 10 + 70 mm, St 11, St 12, St 13 + 50 mm, St 14, St 16, and St 18. The gaps between adjacent segments are designed as 20 mm to prevent the possible contact of the two segments during the test. To avoid flooding, the thin rubber strips are fitted to seal the gaps with some spare room to eliminate the possible load transfer.

Figure 2: The containership model with 14 segments.

Considering the capabilities of wave generation of the wave basin, a scaling ratio of $1:49$ ($\mu = 49$) is chosen, which makes the ship model have available travelling speed, space, and weight margins for fitting in the necessary instrumentation and adjusting the weight distribution. Figure 3 shows the hull offset lines. Table 1 gives the main particulars with two loading conditions of the ship model.

3.2. Mass Distribution of the Ship Model. Table 2 gives the estimation of the mass of each segment of the ship model, which is calculated from the ship mass statistics. The weight distribution of the ship model is also shown in Figure 4. The blue bars demonstrate the mass in the full load condition, and the red bars present the mass in the design draft condition.

3.3. Stiffness Similitude Using Backbone. The similarity of section stiffness is an important step in scaling the full-scale ship to the model. Once the stiffness satisfies a similar criterion, the natural frequency will meet a similar relationship, and its modal shape will be consistent with the full-scale ship. According to the similitude principle, a blue backbone (Figure 5) is designed to simulate the bending of the containership in waves. To satisfy the stiffness similitude of the ship on vertical bending, a kind of steel is chosen to construct the backbone. Young's modulus of steel is 206 Gpa. The Poisson ratio is 0.3. However, the stiffness along the ship length is not uniform. Generally, the inertia moment of the vertical bending at amidships is larger than the values at fore and aft. Therefore, the flexible backbone has been designed to the six variable cross-sections joined end to end. Table 2 gives the design properties of the backbone such as the inertia moment of vertical bending from stern to station 19.

3.4. Construction and Installation of the Backbone. Figure 6 gives the schematic drawing of the installation of the backbone built-in ship model, which is carefully designed. All the hydrodynamic loads transfer to the backbone, which act on the segments. However, the stiffness of the segment did not affect the flexibility of the backbone noticeably. It can be seen that the backbone beam is connected to the ship hull through the transverse supports, which are green, shown in Figure 5.

4. Determination of Modal Property

4.1. Measurement Methods and Instrumentation. It is essential to obtain the modal parameters, including natural frequencies, modal shapes, and damping ratio of the ship model since they are the indispensable input data for hydroelastic analyses. Therefore, both the dry and wet modes, including the vertical bending of the ship model, are measured and analysed in the vibration lab of CSSRC. Before carrying out the modal test, the centre of gravity and inertia of the ship model shall be adjusted to account for full load and design draft loading conditions, respectively.

The modal parameters are determined by a hammering test, hitting the ship model with a soft hammer and recording the vertical vibrations and their decay curves. The roving hammer setup used a PCB-086C04 instrumented hammer for the excitation measurement. The PCB 352C33 accelerometers are employed to measure the dynamic responses of the backbone of the ship model. Figure 7 gives the installation layout of accelerometers, including 30 points for vertical acceleration measurement. The measurement data are obtained and processed by using B&K 3660D, a dynamic data acquisition and processing system. The relevant frequency response function and modal parameters could be derived in the measurement.

To measure the vertical modal shapes, the ship model is suspended in the air by elastic ropes. Figure 8 shows the different suspending patterns on the ropes to measure the vertical modal shapes. In the vertical bending modal measurement, the ropes are going around the side of the hull of the model.

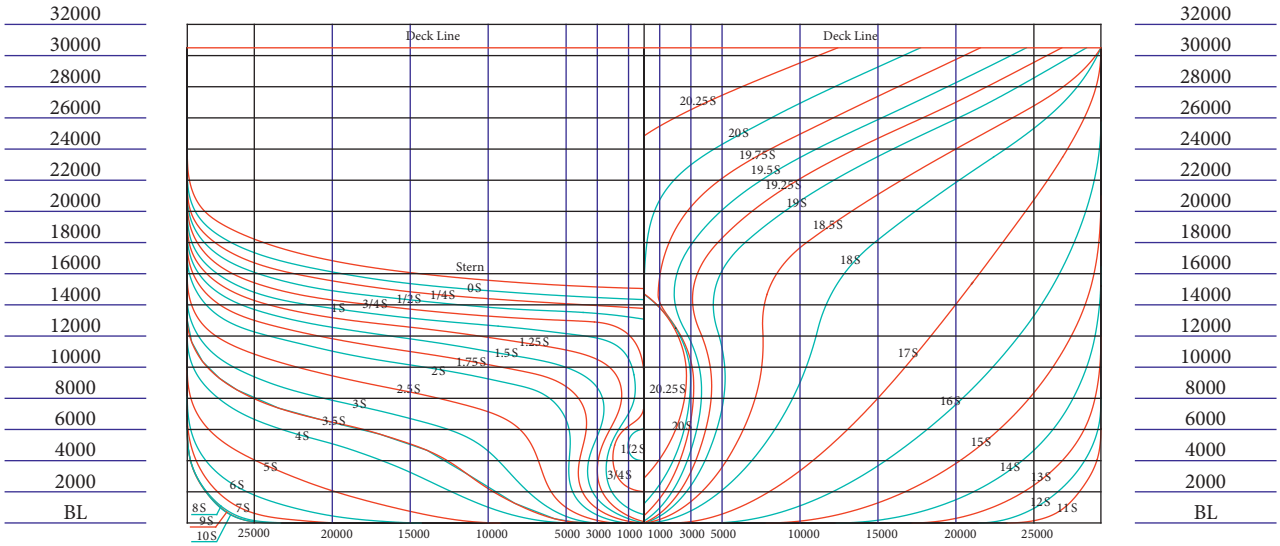

Figure 3: Offset lines of the containership.

Table 1: Main particulars.

Item	Symbol	Ship		Model	
		Full load	Design draft	Full load	Design draft
Scale ration	μ	1	1	49	49
Density of water	ρ (t/m^3)	1.025	1.025	1.000	1.000
Length overall	L_{OA} (m)	399.67	399.67	8.157	8.157
Length between perpendiculars	L_{BP} (m)	383	383	7.816	7.816
Beam	B (m)	58.6	58.6	1.196	1.196
Depth	D (m)	30.5	30.5	0.622	0.622
Draft forward	T_f (m)	15.2	13.37	0.31	0.273
Draft aft	T_a (m)	16.7	15.3	0.341	0.312
Displacement	Δ (t)	260602.9	228482.8	2.161	1.895
Height of CG above baseline	Z_g (m)	27.574	26.106	0.563	0.533
LCG from AP	X_g (m)	182.714	183.485	3.729	3.745
Moment of inertia about y-axis	I_{yy} (kg $\cdot$ m^2)	2.307×10^{12}	1.913×10^{12}	7967.86	6605.7

Table 2: Design properties of the backbone along the ship length.

No.	Length (m)	Outer diameter (m)	Thickness (m)	Inertia moment of vertical bending for one cylinder (m^4)	Inertia moment of vertical bending for two cylinders (m^4)
MI-1	1.1724	0.089	0.005	$1.1679E-06$	$2.3358E-06$
MI-2	0.7816	0.102	0.0055	$1.9472E-06$	$3.8944E-06$
MI-3	3.1264	0.114	0.005	$2.5481E-06$	$5.0963E-06$
MI-4	0.7816	0.102	0.006	$2.0928E-06$	$4.1855E-06$
MI-5	0.7816	0.095	0.005	$1.4358E-06$	$2.8716E-06$
MI-6	0.7816	0.083	0.005	$9.3561E-07$	$1.8712E-06$

It should be noted that the natural frequencies of the mass-spring system in rigid body motion should be well below the elastic deformation resonance modes of the ship model. In addition, the elastic rope shall be hung at the location of vibration modal nodes to minimize the influence of support on the modal results. Before the modal measurement, two kinds of spring rigidity have been employed for comparison, 25537 N/m and 17448 N/m. It is found that the impact of rope rigidity is negligible on the measured results of natural frequency if the model is suspended at modal nodes.

During the vertical modal measurement in the air, the suspension locations are adjusted iteratively until they

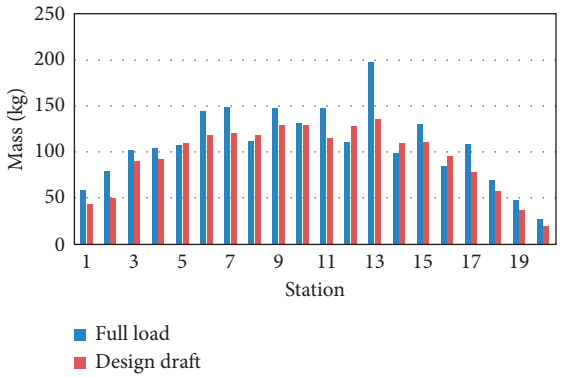

Figure 4: Weight distribution of the ship model.

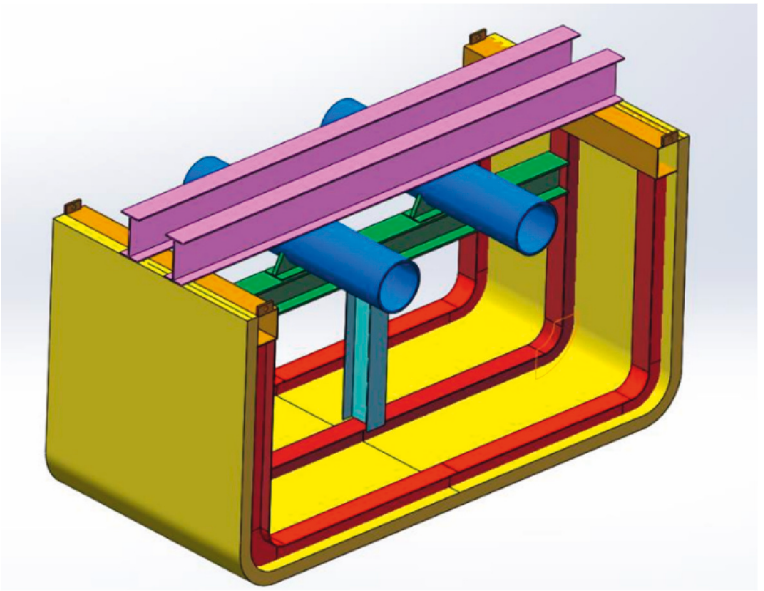

Figure 5: Backbone of the model in blue.

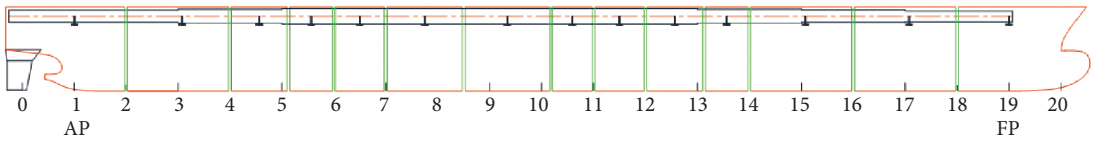

Figure 6: Schematic drawing of the installation of backbone in ship model.

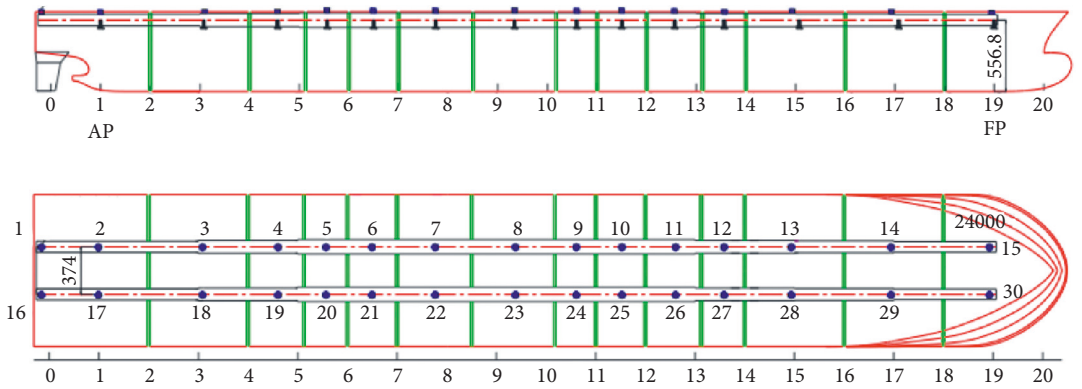

Figure 7: Layout of the accelerometers for modal shape measurement.

Figure 8: Different suspending patterns in the measurement of the modal shapes.

correlated well with the vibration modal nodes derived from the previous measurement analysis.

4.2. Modal Results. The natural frequencies, damping ratio, and modal shape of the model have been analysed from the measurement results. To obtain the resonance frequencies, we plotted the RAOs of accelerations at each measurement point. The RAOs are defined as the ratio of the response amplitude to the amplitude of exciting force. The peaks in these curves indicated the modal resonances of the model.

Figure 9 shows the dry and wet vertical acceleration RAOs at different measured locations under vertical bending (VB) excitation of the ship model for both the full load condition and design draught condition.

Figures 9(a) and 9(b) show the natural frequencies of full load and design draft loading conditions in air respectively. Figures 9(c) and 9(d) show the resonant frequencies of full load and design draft loading conditions in the water.

In Figure 9, we can see that the natural frequencies of the ship model can be investigated clearly. Although the acceleration signals are thirty, the two-node VB and three-node peaks nearly occur at the same frequencies, respectively. It is worth pointing out that there are small peaks before the frequency according to the two-node VB. This is the natural frequency due to the elastic cord in the suspension system. Therefore, the rigidity of the hanging rope selected should avoid the natural frequencies of the ship model. In contrast, the resonant frequency test results in the water show that the peaks are not as sharp as the natural frequency peaks in the air, showing a wider distribution of peaks. The two-node VB and three-node VB peaks are discernible.

Table 3 gives the natural frequencies and damping ratio of the vertical bending mode of the ship from measurement analyses.

From Table 3 we can find that the wet frequencies are lower than the dry frequencies in the same modal shape. It is because of the effect of the added mass in the water. The greater the masses, the lower the frequencies. Similarly, the 2-node frequency in full load is lower than that in design draft loading, the same as the 3-node frequency. In addition, the damping coefficient corresponding to each order frequency is obtained according to the half-power method. As well known, the damping coefficient plays a key role in the peak value of the subsequent hydroelastic wet mode.

In addition, natural frequencies are the inherent properties of ship models in air and water. The uncertainty of the modal test mainly comes from the accuracy of the measuring instrument, the detail of the ship model, and the change in environmental factors. Since a total of 30 acceleration sensors are arranged on the measured backbone, through three repeatability tests, these data are analysed to obtain the standard deviation and measurement uncertainty.

5. Dry Mode and Wet Frequency Prediction

5.1. FEM for Dry Modal Calculation

5.1.1. General Introduction. Due to the lack of the inertia moment of each section, the simplified beam model is not as accurate as a 3D FEM for simulating the moment of inertia of a ship. The 3D numerical model for simulation is modelled by FE analysis software MSC.Patran. Due to the accuracy of the modal calculation, the two backbones are modelled by solid elements. To obtain the inertia moment, the mass and the instruments box are created by solid elements. The girders, ribs, and supports are built in steel by plate elements with different thicknesses. The ship hull is also constructed of plate elements, which are made of fibreglass. The FEM of the containership of full load condition is seen in Figure 10. Some groups of mass cubic are located on the side of the ship model. The whole FEM has 495387 nodes and 315117 elements in the

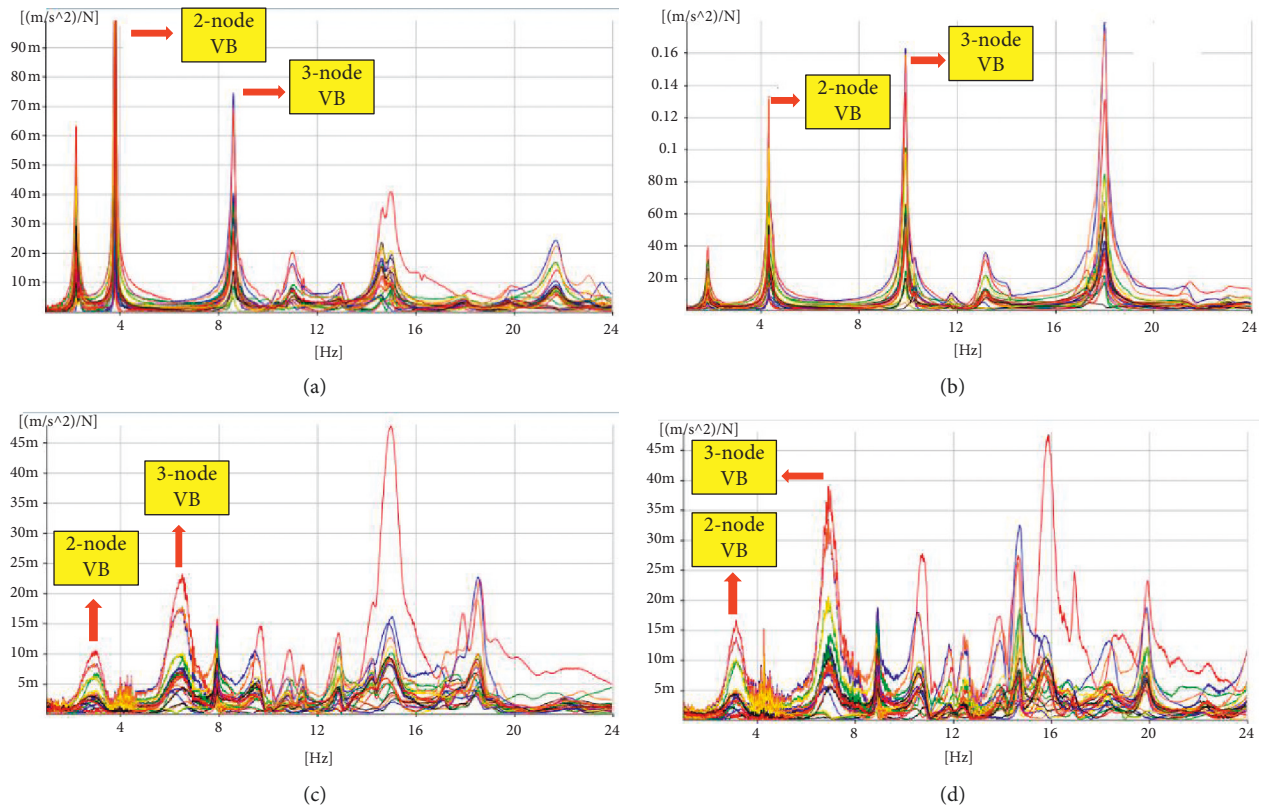

Figure 9: Vertical acceleration RAOs for vertical bending (VB) excitation. (a) Full load condition in air. (b) Design draft loading condition in air. (c) Full load condition in water. (d) Design draft loading condition in water.

Table 3: Vertical bending modal results from measurement.

Loading condition	Modal shape	Dry mode		Wet mode	
		Natural frequency (Hz)	Damping ratio (%)	Natural frequency (Hz)	Damping ratio (%)
Full load	2-Node	3.823	0.23	2.825	6.3
	3-Node	8.575	0.8	6.455	4.0
Design draft	2-Node	4.337	0.93	3.104	5.6
	3-Node	9.923	0.48	6.955	2.5

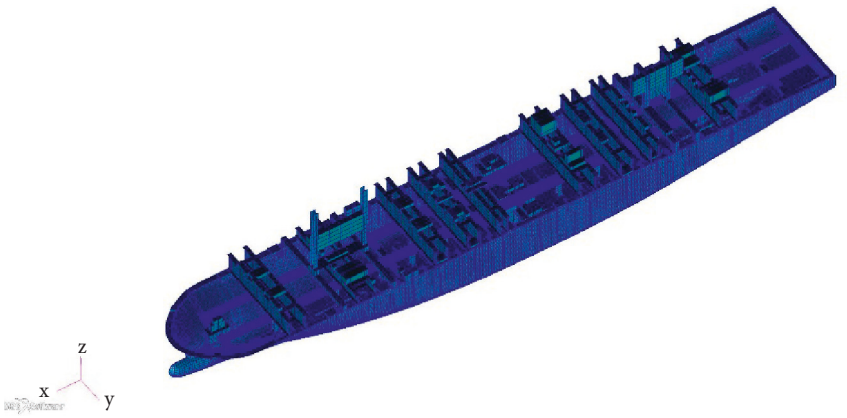

Figure 10: FEM of the containership of full load condition.

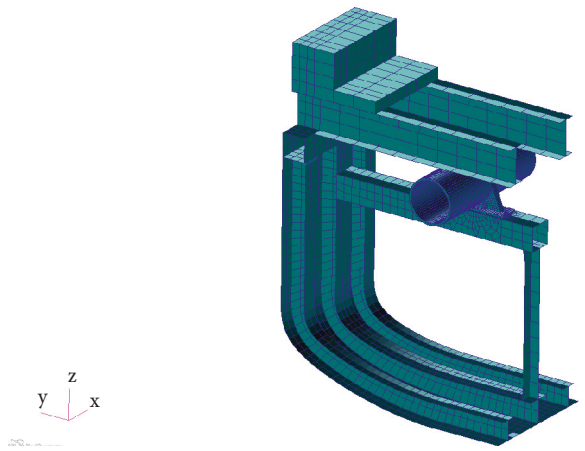

Figure 11: Connection simulation of the backbone to the hull.

Table 4: Comparison of predicted dry and wet natural frequencies in the full load condition.

Mode		Dry mode			Wet mode		
Direction	Modal shape	Test	Cal	Error (%)	Test	Cal	Error (%)
VB	2-Node	3.823	3.766	1.5	2.825	2.785	1.4
VB	3-Node	8.575	8.361	2.5	6.486	6.366	0.5

Table 5: Comparison of predicted dry and wet natural frequencies in design draft condition.

Mode		Dry mode			Wet mode		
Direction	Modal shape	Test	Cal	Error (%)	Test	Cal	Error (%)
VB	2-Node	4.337	4.28	1.4	3.104	2.992	3.6
VB	3-Node	9.923	9.46	4.7	6.955	7.098	2.1

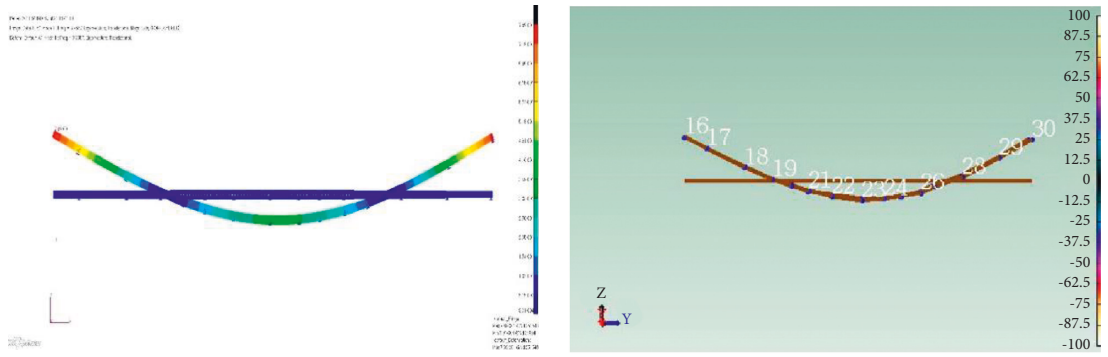

(a) (b)

Figure 12: Vertical bending modal shape (2 nodes), full loading condition. (a) Numerical prediction. (b) Measurement results.

full load condition and 494318 nodes and 314447 elements in the design draft condition.

5.2. Connection Simulation. The elements of the backbone are fixed by transversal supporting, which is connecting to the hull shell from the port side to the starboard as shown in Figure 11.

5.3. Natural Frequency Prediction. Based on the potential theory, the 3D hydroelastic method is employed. The key to the theory of hydroelasticity is the fluid-structure coupling; that is, the force is transmitted through the dry-wet matching relationship between the dry meshes and the wet surface elements. A set of 3742 hydrodynamic panels is modelled to calculate hydrodynamic coefficients, such as added mass, damping coefficient, and exited force. Using the dry–wet element matching, the fluid pressure is loaded on the structural meshes, while the elastic deformation is imposed on the wet panels. The dry and wet natural frequencies of the ship model are predicted for the previously mentioned FEM. The comparisons of the numerical results with the

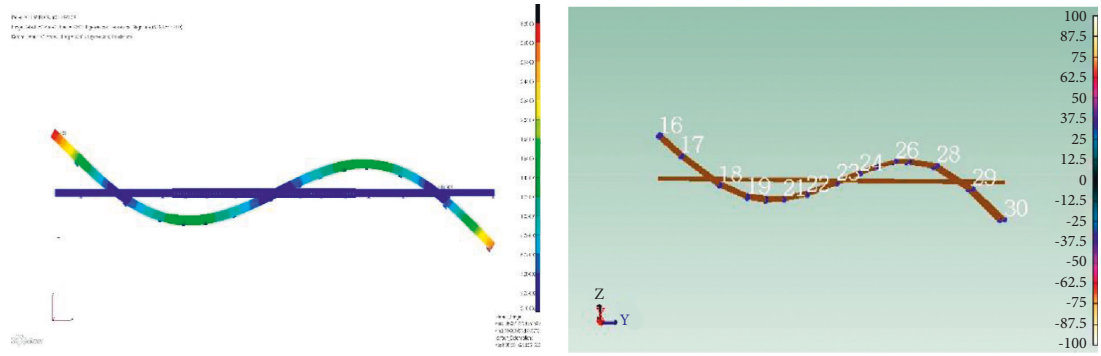

(a) (b)

Figure 13: Vertical bending modal shape (3 nodes), full loading condition. (a) Numerical prediction. (b) Measurement results.

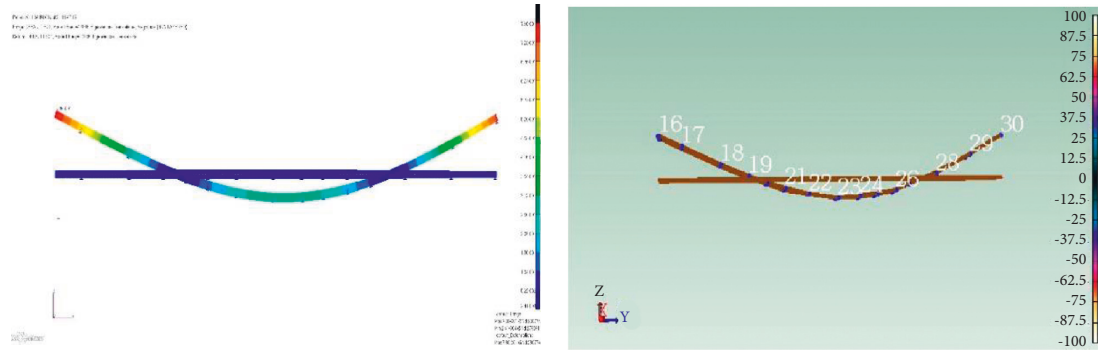

(a) (b)

Figure 14: Vertical bending modal shape (2 nodes), design draft loading condition. (a) Numerical prediction. (b) Measurement results.

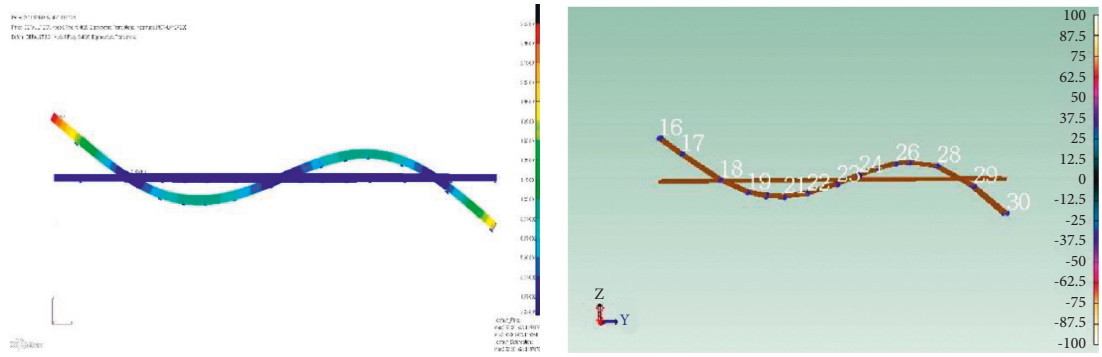

(a) (b)

Figure 15: Vertical bending modal shape (3 nodes), design draft loading condition. (a) Numerical prediction. (b) Measurement results.

measurement results are shown in Tables 4 and 5 for full load and design draft loading conditions. It can be seen that for all the modes very good agreements are achieved both for dry and wet frequencies.

5.4. Modal Shape Prediction. The vertical bending modal shape prediction results are shown in the following figures. The modal shapes derived from modal measurement are also given for comparison. Figures 12-13 show the comparison results of 2-node and 3-node vertical bending shapes in full loading condition, while Figures 14-15 give the comparison of the results of 2-node and 3-node vertical bending shapes in design draft loading condition. Generally speaking, a fairly good agreement has been achieved.

6. Conclusion

In the CSSRC-20,000 TEU JIP, a 20,000 TEU containership with an overall length of about 400 m is designed as the target ship, which will be utilized to carry out a model test in the new seakeeping wave basin of CSSRC and generate

benchmark model test data for comparative studies using most recent numerical methods and software. In this paper, the 1 : 49 scale ship model is briefly introduced, in conjunction with the determination of modal parameters, including natural frequencies, modal shapes, and damping ratio of the ship model, since they are the indispensable input data for hydroelastic analyses.

Through the comparative analysis of modal calculation and test results, the mass distribution and stiffness distribution of the containership model are the basis for obtaining the natural frequency and modal shape. In the finite element numerical modelling, only by simulating the segmental mass of the actual ship model and measuring the stiffness of the backbone, the accurate result of the natural frequency would be obtained. In addition, the simulation of all connections of the ship model will also change the results. However, there are some uncertain factors in the manufacture and installation of the ship model. Furthermore, the stiffness of the suspension rope and the position of the suspension point in the modal test are also factors that affect the results. By checking and eliminating all uncertain factors, the dry and wet modalities of the numerical modal calculation can be consistent with the results of the modal test. Natural frequency and modal observations of the containership model are required to ensure the accuracy of the hydroelastic analysis.

A 3D FEM of the ship is built to carry out modal analysis in a vacuum. From the comparison of the numerical predictions and the hammering test results, it can be concluded that a generally good agreement has been achieved, particularly for the lower-order deflection modes. The FEM corresponding to full load and design draft loading conditions will be distributed to JIP members for further comparative studies of linear and nonlinear hydroelastic analyses.

This article is devoted to the full exposition of the modal tests necessary for the hydroelastic analysis of large containerships. Therefore, hydroelastic effects can be seen in the elastic vibration frequencies and modes of the containership model. The wet mode of the containership model is obtained through hydrodynamic analysis. By comparing with the test results, the position and shape of the resonance frequency that causes the ship's hydroelasticity can be observed more clearly.

Data Availability

The data used to support the findings of this study are included in the article. The basic data can be found at jip.cssrc.com.

Conflicts of Interest

The authors declare that they have no conflicts of interest.

Acknowledgments

This research work was supported by the National Natural Science Foundation of China, PR China (51809241), CSSRC-20, 000TEU JIP, and the High-Tech Ship Research Projects Sponsored by MIIT.

References

[1] A. D. Papanikolaou and T. E. Schellin, "A three-dimensional panel method for motions and loads of ships with forward speed," *Journal for Research in Shipbuilding and Related Subject*, vol. 39, no. 4, pp. 145–156, 1992.

[2] Y. Welaya, T. M. Ahmed, and H. S. Wahab, "A linear three-dimensional frequency-domain numerical model for the prediction of ship motions in regular/irregular seaways," *Towards Green Marine Technology and Transport*Taylor & Francis Group, Milton Park, Oxfordshire, UK, pp. 167–174, 2015.

[3] J. Jiao, S. Huang, S. Wang, and C. Guedes Soares, "A CFD–FEA two-way coupling method for predicting ship wave loads and hydroelastic responses," *Applied Ocean Research*, vol. 117, Article ID 102919, 2021.

[4] P. A. K. Lakshmynarayanana and S. Hirdaris, "Comparison of nonlinear one- and two-way FFSI methods for the prediction of the symmetric response of a containership in waves," *Ocean Engineering*, vol. 203, pp. 1–17, Article ID 107179, 2020.

[5] J.-H. Kim and Y. Kim, "Numerical analysis on springing and whipping using fully-coupled FSI models," *Ocean Engineering*, vol. 91, pp. 28–50, 2014.

[6] I. Senjanović, N. Vladimir, N. Hadžić, and M. Tomić, "Beam structural modelling in hydroelastic analysis of ultra large container ships," *Recent Advances in Vibration Analysis*, University of Ottawa, Ottawa, Canada, pp. 193–222, 2011.

[7] S. Malenica and Q. Derbanne, "Hydro-structural issues in the design of ultra large container ships," *International Journal of Naval Architecture and Ocean Engineering*, vol. 6, no. 4, pp. 983–999, 2014.

[8] S. E. Hirdaris, Y. Lee, and G. Mortola, "The influence of nonlinearities on the symmetric hydrodynamic response of a 10,000 TEU Containership," *Ocean Engineering*, vol. 111, pp. 166–178, 2016.

[9] W. Ye, G. Yu, and X. Lu, "Hydroelastic analysis of container ships," *Vibration and Shock*, vol. 2, pp. 69–71, 1995.

[10] Y. Lin, H. Guo, and G. Yang, "Research on the hydroelastic effect of ultra large container ships," *Ship Engineering*, vol. 37, no. s2, pp. 15–19, 2015.

[11] Y. Chen, "Practical calculation methods of wave-induced vibration and whipping effects in ship design. In memory of Academician Binghan Xu," in *Proceedings of the Conference on Ship and Ocean Structure Mechanics*, Wuxi, China, 2011.

[12] Y. Han, L. Chen, and W. Wang, "Structure design of ultra-large container ship," *Ship and Ocean Engineering*, vol. 31, no. 04, pp. 10–17, 2015.

[13] Z. Zhang, L. Dandan, and L. Yan, "Research on the influence of wave-induced vibration on the fatigue strength of ultra-large container ships," *China Shipbuilding*, vol. 60, no. 1, pp. 1–10, 2019.

[14] I. Senjanović, S. Malenica, and S. Tomas, "Investigation of ship hydroelasticity," *Ocean Engineering*, vol. 35, no. 5-6, pp. 523–535, 2008.

[15] I. Senjanović, S. Malenica, and S. Tomašević, "Hydroelasticity of large container ships," *Marine Structures*, vol. 22, no. 2, pp. 287–314, 2009.

[16] W. Wang and C. Guedes Soares, "Review of ship slamming loads and responses," *Journal of Marine Science and Application*, vol. 16, no. 4, pp. 427–445, 2017.

[17] Y. Wu, R. Z. Chen, and J. Lin, "Experimental technique of hydroelastic ship model," in *Proceedings of the 3rd International Conference on Hydroelasticity in Marine Technology*, pp. 131–142, Oxford, UK, September 2003.